

Accepted Manuscript

Title: A partly stage-structured model for the abundance of salmon lice in salmonid farms

Author: Aldrin M. Jansen P.A. Stryhn H.

PII: S1755-4365(18)30070-7

DOI: <https://doi.org/doi:10.1016/j.epidem.2018.08.001>

Reference: EPIDEM 311



To appear in:

Received date: 17-4-2018

Revised date: 12-7-2018

Accepted date: 16-8-2018

Please cite this article as: Aldrin M., Jansen P.A., Stryhn H., A partly stage-structured model for the abundance of salmon lice in salmonid farms, *EPIDEMICS* (2018), <https://doi.org/10.1016/j.epidem.2018.08.001>

This is a PDF file of an unedited manuscript that has been accepted for publication. As a service to our customers we are providing this early version of the manuscript. The manuscript will undergo copyediting, typesetting, and review of the resulting proof before it is published in its final form. Please note that during the production process errors may be discovered which could affect the content, and all legal disclaimers that apply to the journal pertain.

A partly stage-structured model for the abundance of salmon lice in salmonid farms

Aldrin, M.^{a*}, Jansen, P.A.^b, Stryhn, H.^c

^a Norwegian Computing Center, P.O.Box 114 Blindern, N-0314, Oslo, Norway

^b Norwegian Veterinary Institute, P.O. Box 750 Sentrum N-0106, Oslo, Norway

^c University of Prince Edward Island, 550 University Avenue, Charlottetown,

Prince Edward Island, Canada C1A 4P3

* Corresponding author: Tel: +47 22 85 26 58, fax: +47 22 69 76 60,

Email address: magne.aldrin@nr.no

July 12, 2018

Abstract The parasitic salmon louse constrains growth in the Norwegian salmon farming industry through density dependent host-parasite interaction. Hence, there is a need for insight into how increases in salmon production, varying spatial organisation of the production and pest control strategies affect salmon louse population dynamics. Here we present a new salmon louse model for exploring effects of varying salmon farming conditions on spatio-temporal abundances of the parasite. The salmon louse model is partly stage-structured, comprising of i) adult female lice and ii) other mobile stages of lice. The abundance of adult

13 females depend on survival of females from previous weeks and recruitment from
 14 the other mobile group of lice. The other mobiles also depend on survival of other
 15 mobiles from previous weeks, as well as recruitment from the previous generation
 16 of reproducing adult females from the same farm or from farms in the neighbour-
 17 hood. In addition, expected abundances of the two stage-groups are modelled
 18 as functions of biological and physical covariates. The model is fitted to weekly
 19 salmon farm data covering all marine farms producing salmonids along the Nor-
 20 wegian coast over the years 2012-2016. Among novel results from fitting the model
 21 are estimates of the time-lag structure representing recruitment of other mobile
 22 lice from the previous generation adult females for different temperatures. Fur-
 23 thermore, the model estimates how various factors affect the susceptibility of fish
 24 on farms to louse infection and effects of treatments to control infection. Finally,
 25 the model estimates density dependent effects of increasing the number of fish in
 26 farms and of increasing the numbers of farms, on the rate of recruitment of other
 27 mobile lice. Analytically, the parameters representing density dependencies sug-
 28 gest that few farms with many fish and large between farm distances is effective
 29 in terms of minimising the overall output of salmon lice infection.

30 KEY WORDS: Salmon lice; stage-structured model; aquaculture

31 $\vec{i} \gg \vec{j}$

32 **1 Introduction**

33 Farming of salmonids has grown to become one of the major export industries in
 34 Norway. The parasitic salmon louse, however, threatens the sustainability of the
 35 salmon farming industry (Taranger et al., 2015). In particular, the salmon louse,

36 *Lepeophtheirus salmonis*, constrains growth in the Norwegian salmon farming
 37 industry due to large scale host-parasite density dependence (Jansen et al., 2012;
 38 Kristoffersen et al., 2017). As an instrument to promote sustainable growth in
 39 the industry, the Norwegian coast was recently divided into 13 production-zones
 40 in which environmental criteria will determine future growth in the production of
 41 farmed salmonids. For the time being, the only criterion to decide future growth
 42 in salmon production within the production-zones is the local burden of salmon
 43 lice (Kristoffersen et al., 2017). The reasoning behind this is that spillover of
 44 salmon lice from farmed salmon represents a major threat to the viability of
 45 wild salmonid stocks, and that there is a density dependent association between
 46 farmed salmon hosts and the abundance of the salmon louse parasite (Forseth
 47 et al., 2017; Jansen et al., 2012). Accordingly, there is a strong incentive for
 48 the salmon farming industry to reduce salmon lice infections in salmon farms.
 49 Numerous new control methods and control strategies are adopted, with costs of
 50 louse control accelerating (Abolofia et al., 2017; Liu and Bjelland, 2014), but with
 51 limited insight into the cost-efficiency of various preventive actions. The latter
 52 is especially true when considering scales of multiple farms interacting through
 53 between farm spread of infectious lice (Aldrin et al., 2013). Key questions in this
 54 regard are how the population dynamics of the salmon louse will be affected by
 55 increasing production of farmed salmonids, the spatial organisation of farms or
 56 pest control strategies.

57 Exploring these questions is not simply a question of comparing different areas
 58 or different periods of production since each sample of the production history is
 59 the product of its own set of conditions. However, if you are able to implement
 60 the major driving forces for the host-parasite population dynamics in a predic-
 61 tive model, you can explore such questions in simulation experiments (Tildesley

et al., 2012; Brooks-Pollock et al., 2014; Pettersen et al., 2016). The Norwegian farmed salmon host and louse parasite association is well suited for this approach. Due to strict regulations of this production system, a wealth of data are reported to document farm populations of salmonids, abundances of parasites on these fishes, environmental data and anti-parasitic treatments, in space and time. Furthermore, farm management determines salmonid host population dynamics in this system. This means that we only need to model the parasite population, whereas the host population can be pre-determined. Finally, due to the massive dominance of farmed salmonids over wild salmonids in coastal areas of Norway (Jansen et al., 2012; Torrissen et al., 2013), it is reasonable to neglect any contribution from hosts other than farmed salmonids to the population dynamics of the salmonid specific salmon louse.

Thus motivated, the main goal in the present study is to develop a simulation model for exploring effects of varying farming conditions on spatio-temporal abundances of salmon lice on farmed salmon along the Norwegian coast. Variable farming conditions could be production volumes, the location of farms or pest management strategies. The salmon-lice model is partly stage structured, comprising of i) adult female lice and ii) other mobile stages of lice. Other mobiles consist of parasitic pre-adult stages and adult males, all capable of moving about on fish hosts. The expected abundances of the two stage-groups on farmed salmonids are modelled as functions of biologically motivated co-variables. Essentially, the adult females for a given week and farm depend on the survival of females from previous weeks and recruitment of females from the other mobile group of lice.

We do not anticipate that parasitic lice spread naturally between hosts (Hamre

et al., 2013). Although it has been suggested that parasitic lice may be spread in conjunction with anti-parasitic treatments, we restrict recruitment into adult females to be from other mobiles on the same fish and farm. The other mobiles depend on survival of other mobiles from previous weeks at the same farm. Recruitment into this group of stages, however, depends on reproduction from the prior generation adult females, along with the planktonic spread of infectious copepodites (Hamre et al., 2013). These recruits may therefore come from the same farm or from farms in the neighbourhood. For neighbourhood farms we scale the relative contribution according to seaway distance to the given neighbourhood farm using a function with parameters estimated from the data. All biological processes in the two sub-models are subject to temperature dependency. Furthermore, farms are subject to pest control in the form of anti-parasitic treatments with instant effects. The susceptibility of the fish in a farm to lice infection depends on fish size, the numbers of fish on the farms and other covariates. The sub-models for adult females and other mobiles are fitted to farm data on a weekly resolution covering all marine farms producing salmonids along the Norwegian coast over the years 2012 - 2016.

In this paper, we first present the data on reported louse abundances and farmed fish populations. We go on to present the sub-models for the two stage-groups of lice. We continue by defining how we account for correlations in the time-series data of the two stage-groups, in order to calculate correct uncertainty in forecasts from the model. In the results and discussion sections, we present parameter-estimates for the two sub-models and discuss important aspects with regard to the population dynamics of salmon lice on farmed salmonids. Among such aspects, we explore i) the contribution of various time-lags of adult female lice to the recruitment into the stage-group of other mobiles; ii) how various covariates affect

the susceptibility of the fish on a farm; iii) and how host density dependence affects the expected abundances of the two stage-groups one week ahead under standardised conditions. Finally, we illustrate how the model performs when used for predicting louse abundances one to eight weeks ahead.

2 Materials and methods

The present study-system consists of marine farms in coastal waters of Norway nurturing salmonids in open water net-pens. The fish are typically stocked as smolts produced in freshwater farms and on-grown for roughly 18 months, until slaughtering for food consumption. During the marine on-growing phase, the fish are exposed to infectious salmon louse copepodites that are spread about as plankton in the water current. To approximate this spread we use a distance based relative risk function estimated from the data. This does not account for water currents, but can be regarded to represent the normalised spread of the planktonic salmon lice between farms in the present data set, regardless of the environmental conditions that force water currents. Once attached to a fish, the copepodites develop through two larval stages attached to the fish, two pre-adult mobile stages and finally adult males and females who reproduce the next generation planktonic stages (Hamre et al., 2013). More detailed descriptions of salmon farming and the salmon louse parasite appear in previous papers (Jansen et al., 2012; Aldrin et al., 2013).

133 2.1 Data

134 The data used for the present study consists of i) farm locations, collated from an
 135 open source Aquaculture register hosted by the Norwegian Directorate for Fish-
 136 eries (Anonymous, 2017a). From these data we have calculated pairwise seaway
 137 distances between all farms, but truncated at 100 km (Jansen et al., 2012). Farm
 138 populations of fish ii), i.e. total numbers of fish, fish size and species (Atlantic
 139 salmon, *Salmo salar*, or rainbow trout, *Onchorhynchus mykiss*). These data are re-
 140 ported on a monthly frequency, but are not publicly available due to stock marked
 141 sensitivity. The farm population data are available to The Norwegian Veterinary
 142 Institute for surveillance and research purposes, through the responsible Norwe-
 143 gian Food Safety Authority (Jansen et al., 2012). Salmon louse related data iii),
 144 i.e. abundances of adult females and other mobiles of salmon lice reported from
 145 lice counts, anti-parasitic treatments and water temperatures. Counting of lice
 146 and reporting is done on a weekly frequency and these data are now publicly
 147 available (Anonymous, 2017b).

148 The present data include all 991 Norwegian marine fish farms with standing
 149 stocks of either Atlantic salmon or rainbow trout (salmonids) in any week from
 150 week 1 in 2012 to week 44 in 2016. The data from the first sixteen weeks were
 151 only used to construct lagged explanatory variables, whereas the model was fitted
 152 to data from the 17th week in 2012 and onward. In the following description, we
 153 therefore only summarise data from the latter period. The number of active farms
 154 was then reduced to 979. Each salmonid farm normally had several consecutive
 155 periods of fish production, interrupted by periods of fallowing (i.e. no fish on
 156 the farm). Each farm could produce either Atlantic salmon or rainbow trout, or
 157 both species at the same time. The fish population within a production period

is termed a cohort and the present data consists of 2 598 cohorts with a total of 137 595 farm-weeks of fish production. Farms produced between one and seven consecutive cohorts. For each salmonid farm, it is obligatory to report the salmon lice abundance on a sample of fish to the responsible Norwegian Food Safety Authority. We assumed that the number of sampled fish was always 40, corresponding to ten fish sampled from each of four cages, which is the minimum required sample size for a farm of normal size with eight cages (Jansen et al., 2012). The reported salmon lice abundances were therefore multiplied by 40 and implemented as the response variable in the present model. In reality, the number of sampled fish was probably often larger than 40, but this did not necessarily affect the mean number of lice per fish. However, lice abundance data were missing for about 16% of the total number of weeks with farmed fish, giving 115 132 farm-weeks with reported salmon lice abundance. The number of missing lice counts is particularly high during the first weeks after stocking, since the fish should be disturbed as little as possible in this period and because the lice abundance is expected to be low. Ignoring the first four weeks of each cohort, the proportion of missing lice data was reduced to 13%.

Lice abundances were recorded for both for adult females (A) and other mobile stages of lice (O). The A category include adult females with and without egg strings attached. The O category include adult males and pre-adult stages of both males and females. The abundance of adult females was between 0 and 1.2 in 95% of the farm-weeks, with a mean of 0.18 lice per fish (Table 1). The distribution of adult female abundance was profoundly right-skewed, being exactly 0 in 41% of the farm-weeks, whereas the highest reported abundance was 29 lice per fish. The abundance of other mobiles was higher than for adult females, with a mean of 0.82 lice per fish, and being 0 in 17% of the farm-weeks. Summary statistics

for lice abundance and several other quantities are found in Table 1.

Table 1: Summary statistics for various quantities over all weeks (over all farms for No. neighbouring farms) with observed values of the quantity in question.

Quantity	Unit	Mean	2.5% percentile	97.5% percentile	Minimum	Maximum
A abundance in sample	lice per fish	0.18	0.00	1.23	0.00	29.5
O abundance in sample	lice per fish	0.82	0.00	5.15	0.00	86.6
No. fish	millions	0.700	0.028	1.81	0.00021	5.10
Average weight of fish	kg	2.4	0.117	6.6	0.029	15.0
Proportion of salmon*	%	93	0	100	0	100
Seawater temperature	°C	9.3	3.4	16.2	0.1	22.6
No. neighbouring farms within 10 km		4.3	0	6	0	18

A: Adult females

O: Other mobiles

*: Farmed salmonids being Atlantic Salmon

The black curves in Figure 1 show how the observed lice abundances vary over the data period averaged over all farms and for two selected farms. The lice counts have a clear seasonal pattern driven by the seawater temperature.

Figure 2 shows the locations of all Norwegian salmonid farms that actively produced salmonids any week during the study period, with a closer look at farms that were active in autumn 2013 (week 44) in an area in the South-West of Norway.

The seawater temperature was missing for 7.7% of the farm-weeks. Each missing temperature was imputed by a weighted mean of all observed temperatures the same week, with weights proportional to the inverse of the seaway distance to the current farm with the missing temperature. For 1.4% of the farm-weeks, there were no fish at the same farm in the previous week, and for 3/4 of these weeks, the mean fish weight was less than 250 g. This indicates that the fish cohort was stocked for the first time on the given farm, whereas a start weight

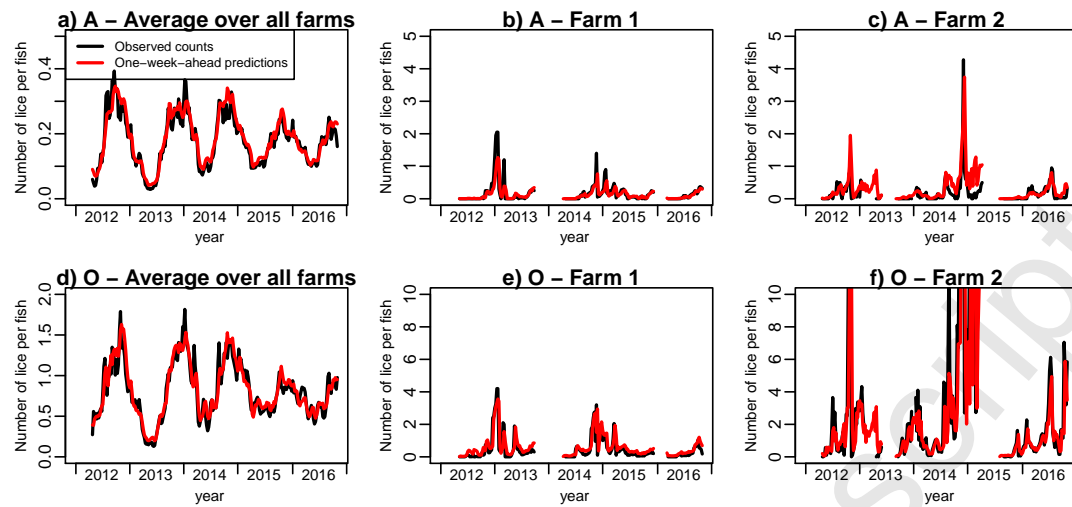


Figure 1: Time plots of observed counts (black) and one-week-ahead predictions (red) of the abundance of adult females (upper panels) and other mobiles (lower panels) in average over all farms (panels a and d), and for two separate farms (panels b, c, e and f).

of 250 g or larger indicates that the fish cohort had been relocated, i.e. moved from another marine farm. Medical salmon lice treatments were applied in 4.3% of the farm-weeks.

In addition, the use of non-medical treatments and novel methods to shield farmed fish from infection has increased towards the end of the data-period. Shielding methods include the use of plankton nets surrounding the net pens, whereas non-medical treatments include mechanical removal of lice, or the use of warm- or fresh-water. The present model does not account for this since we lack sufficient data. For the same reason, we do not account for the use of cleaner fish to control lice, although this has been shown to have an effect in a more detailed data set (Aldrin et al., 2017). Finally, we have also ignored effects of salinity since we lack sufficient data, although salinity is known to affect the infection process of salmon lice (Bricknell et al., 2006).

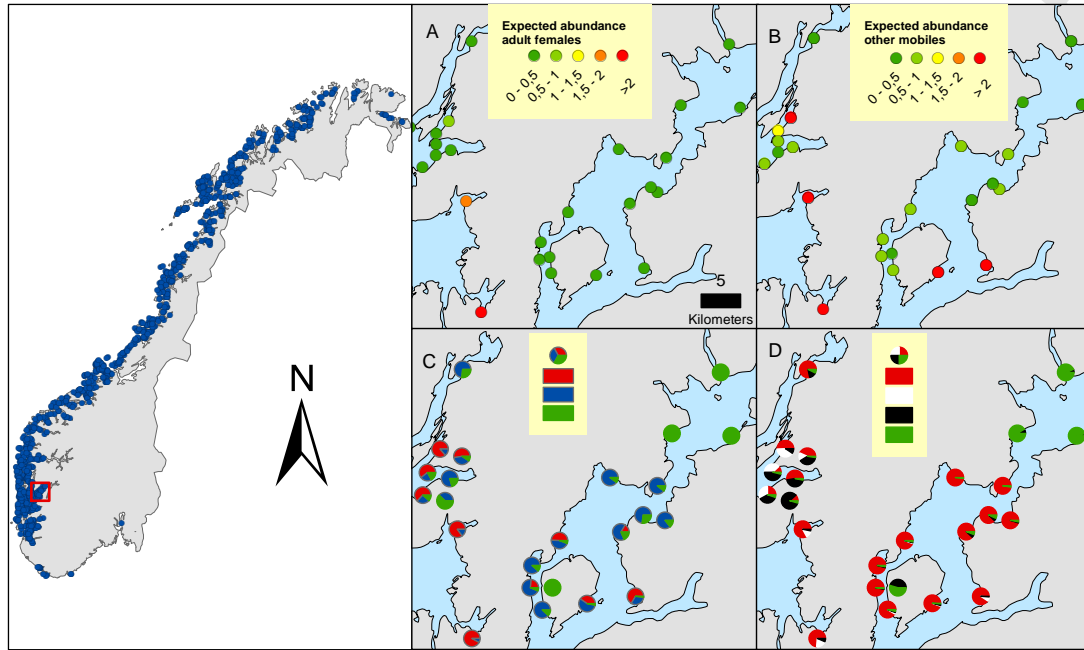


Figure 2: The left panel shows Norway with all farms having reported lice at some time during the data-period 2012-2016 (blue circles). The red square shows the area enlarged in panels A-D. The top panels show the model's expected abundances of adult female lice (A) and other mobiles (B) in farms for week 44 in 2013. The lower panels show pies representing the proportional contribution of various additive sources of infection comprising the model expected abundances in the top panels. For panel C, red colour represents surviving adult female lice; blue represents adult females developed from other mobiles; and green represents non-observed adult females. For panel D, red colour represents surviving other mobiles; white represents recruitment of other mobiles from the prior generation adult females within the same farm; black represents recruitment of other mobiles from the prior generation adult females in neighbouring farms; and green represents non-observed other mobiles (note that some farms have been slightly moved in the lower panels to avoid overlapping symbols).

212 2.2 Model

213 2.2.1 Model structure common for both adult females and other mo- 214 biles

215 The present salmon lice model consists of two sub-models, one for adult females
216 and one for other mobiles. They share some of the same model-structure, but
217 have separate parameter estimates. Let y_{it} denote the counted abundance of lice
218 in a given stage at farm i in week t , that is, either $y_{it} = y_{it}^A$ for adult females or
219 $y_{it} = y_{it}^O$ for other mobiles. This is the average number of lice in the respective
220 stage counted on n fish, where $n = 40$ (as discussed in the previous section).
221 We first present the model structure that is common for adult females and other
222 mobiles, and then present the stage-specific parts of the models. Let further μ_{it}
223 denote the expected abundance, i.e. $\mu_{it} = E(y_{it})$. This expectation is modelled
224 as a function of i) observed lice abundances in previous weeks at the current
225 farm, ii) observed lice abundances in previous weeks at neighbouring farms, and
226 iii) other factors such as seaway distance.

227 We define $n \cdot y_{it}$, the total number of lice (in either stage A or O) counted on n
228 fish, as our response variable, and model it as a zero-inflated, negative binomially
229 distributed variable (Zuur et al., 2009) with expectation $n \cdot \mu_{it}$. Let p_{it}^z denote the
230 probability of excess zero observations in this compound distribution. Thus, y_{it}
231 comes from a negative binomial distribution with probability $1 - p_{it}^z$, and has an
232 excess zero value with probability p_{it}^z . Let further μ_{it}^{NB} denote the expectation in
233 the negative binomial part of the distribution. Then, the expectation of y_{it} can

234 be expressed as

$$E(n \cdot y_{it}) = n \cdot \mu_{it} = (1 - p_{it}^z) \cdot \mu_{it}^{NB}. \quad (1)$$

235 Our main focus is on modelling the expected salmon lice abundance μ_{it} , and we
 236 give a detailed description of the two sub-models for μ_{it} , one for adult females
 237 and another for other mobiles, in the next subsections. The probability of excess
 238 zero observations, p_{it}^z , is also modelled as a function of μ_{it} . From Eq. (1), the
 239 expectation in the negative binomial part of the compound distribution is given
 240 as $\mu_{it}^{NB} = n \cdot \mu_{it} / (1 - p_{it}^z)$. The variance of the negative binomial distribution
 241 can be written as $\mu_{it}^{NB} + (\mu_{it}^{NB})^2 / \nu_{it}$, where $\nu_{it} > 0$ controls the over-dispersion
 242 and is here modelled as a function of μ_{it} . The parameter ν_{it} is sometimes called
 243 a heterogeneity or aggregation parameter and has often been denoted k in par-
 244 asitological literature (Grenfell et al., 1995; Irvine et al., 2000). We present the
 245 models for p_{it}^z and ν_{it} in the Supplementary material, since these only affect the
 246 shape of the distribution of y_{it} , which is not our focus here.

247 The motivations for using a zero-inflated, negative binomial distribution are that
 248 i) it allows for over-dispersion due to large variability from fish to fish, and ii) that
 249 previous analyses of similar data showed that there was an excess frequency of
 250 zeroes (Jansen et al., 2012; Aldrin et al., 2013) compared to a negative binomial
 251 distribution, and including zero-inflation therefore gave a better fit to the data
 252 in those studies as well as in the present one.

2.2.2 The expected lice abundance for adult females

The model for the expected abundance of adult females at farm i in week t has the following additive-multiplicative form:

$$\mu_{it}^A = S_{it} \cdot \kappa_{it}^{susc} \cdot \kappa_{it}^{treat} \cdot (\lambda_{it}^{As} + \lambda_{it}^{Od} + \lambda_{it}^{int}), \quad (2)$$

where all terms are non-negative.

The three multiplicative terms in Eq. (2) are:

- S_{it} is an “at-risk” indicator that is 1 when farm i is active (has a positive number of farmed fish) at week t and 0 otherwise.
- κ_{it}^{susc} is a factor proportional to the susceptibility of farm i . It depends on explanatory variables that characterise the conditions for the fish at farm i at week t , for instance seawater temperature. It has the form

$$\kappa_{it}^{susc} = \kappa^{susc\bullet} \cdot \exp\left(\sum_k \beta_k^{susc} x_{ikt}^{susc}\right), \quad (3)$$

where x_{ikt}^{susc} denotes the k -th explanatory variable for farm i at week t and β_k^{susc} denotes the corresponding regression coefficient. The explanatory variables are centred at given reference values close to the average of each variable, such that the parameter $\kappa^{susc\bullet}$ is the value of κ_{it}^{susc} when all the explanatory variables are equal to their reference values. Specifically, this means when the time is week 30 in 2014, the seawater temperature is 9°C, the farm is located at latitude 64° north, the fish weight is 2 kg and the fish are neither stocked or relocated in week t , see also Table 2. We will also later use the symbol \bullet in the superscript for parameters that represent

a “standard” value of a quantity when modifying explanatory variables are at given reference values.

• κ_{it}^{treat} is a factor that accounts for mortality due to medical treatments, which is modelled as

$$\kappa_{it}^{treat} = 1 - \theta^{tm} \cdot I_{i(t-1)}^t, \quad (4)$$

where θ^{tm} is a parameter representing the treatment mortality and $I_{i(t-1)}^t$ is an indicator variable that is 1 if a treatment has been applied in week $t - 1$ at farm i and 0 otherwise. With this formulation, the treatment effect is assumed to occur the week after the treatment was carried out. This is supported by the data, but see the Supplementary material for a more flexible formulation. Since the mortality parameter θ^{tm} must be between 0 and 1, another unrestricted parameter θ^{tm*} is modelled on the logit scale and θ^{tm} is given by $\theta^{tm} = \exp(\theta^{tm*}) / (1 + \exp(\theta^{tm*}))$.

The three additive terms represent three possible sources of lice infection:

1. λ_{it}^{As} is based on counts of adult females in the two previous weeks within the farm of interest, and represents *adult females* that have *survived* from previous weeks, see details below.
2. λ_{it}^{Od} is based on counts of other mobiles in the two previous weeks within the farm of interest, and represents *other mobiles* that have *developed* into adult females, see details below.
3. λ_{it}^{int} is an *intercept* that, when multiplied by $S_{it} \cdot \kappa_{it}^{susc} \cdot \kappa_{it}^{treat}$, represents the expected abundance of adult females when the counted numbers of both

adult females and other mobiles previous weeks are zero. This term must be included because lice may be present in previous weeks even if the counts of adult females and other mobiles are zero.

Details on how each of these terms are modelled are given in the following:

Surviving adult females are modelled as

$$\lambda_{it}^{As} = \varphi_1^{As} \cdot y_{i(t-1)}^{A*} + \varphi_{2it}^{As} \cdot y_{i(t-2)}^{A*} \cdot S_{i(t-1)}, \quad (5)$$

where:

- $y_{i(t-l)}^{A*} = \left(y_{i(t-l)}^A\right)^\alpha$, where α is a positive parameter that allows for a non-linear dependency of the previous weeks' lice counts.
- $\varphi_1^{As} = 1$ is an autoregressive coefficient set to 1 for identifiability, since this coefficient is statistically confounded with the factor $\kappa^{susc\bullet}$ in (3).
- φ_{2it}^{As} is another positive autoregressive coefficient that depends on the seawater temperature, and therefore varies by time, through the following equation

$$\varphi_{2it}^{As} = \varphi_2^{As\bullet} \cdot \exp(\beta_2^{As} \cdot (T_{it} - 9)), \quad (6)$$

where $\varphi_2^{As\bullet}$ and β_2^{As} are parameters and $T_{it} - 9$ is the seawater temperature centred around 9°C.

- $S_{i(t-1)}$ has the same definition as before, and is included to ensure that lice from time $t - 2$ cannot survive until time t if the farm is inactive the week in between.

311 The term representing *other mobiles developed* into adult females is modelled as

$$\lambda_{it}^{Od} = \varphi_{1it}^{Od} \cdot y_{i(t-1)}^{O*} + \varphi_{2it}^{Od} \cdot y_{i(t-2)}^{O*} \cdot S_{i(t-1)}, \quad (7)$$

312 where:

- 313 • $y_{i(t-l)}^{O*} = \left(y_{i(t-l)}^O \right)^\alpha$.
- 314 • φ_{1it}^{Od} is an autoregressive coefficient, depending on the seawater temperature
315 in the same way as φ_{2it}^{As} in Eq. (6), but with parameters $\varphi_1^{Od\bullet}$ and β_1^{Od} , where
316 $\varphi_1^{Od\bullet}$ is the autoregressive coefficient when the seawater temperature is 9°C.
- 317 • φ_{2it}^{Od} is another autoregressive coefficient, also depending on the seawater
318 temperature in the same way as φ_{2it}^{As} in Eq. (6), but with parameters $\varphi_2^{Od\bullet}$
319 and β_2^{Od} .

320 The *intercept*, λ_{it}^{int} , representing the scaled expected abundance when the counted
321 numbers of lice previous weeks are zero, is modelled as a function of the seawater
322 temperature in the same way as φ_{1it}^{Od} in Eq. (6), but with parameters $\lambda^{int\bullet}$ and
323 β^{int} .

324 The coefficients φ_{2it}^{As} , φ_{1it}^{Od} , φ_{2it}^{Od} and λ_{it}^{int} , which depend on seawater temperature,
325 can be interpreted relative to the fixed value of $\varphi_1^{As} = 1$. However, because all of
326 these are multiplied by κ_{it}^{usc} , which also depends on seawater temperature, the
327 net temperature dependency is more complex.

2.2.3 The expected lice abundance for other mobiles

The model for the expected abundance of other mobiles at farm i in week t has the following additive-multiplicative form:

$$\mu_{it}^O = S_{it} \cdot \kappa_{it}^{susc} \cdot \kappa_{it}^{treat} \cdot (\lambda_{it}^{Os} + \lambda_{it}^{Adw} + \lambda_{it}^{Adn} + \lambda_{it}^{int}), \quad (8)$$

where again all terms are non-negative. Below, we only explain terms that are different from the model for adult females. Other terms, with the same notation as in the model for adult females, have the same structure and interpretation as in that model, but different parameter values. The terms that differ from the model for adult females are:

1. λ_{it}^{Os} based on counts of other mobiles in the two previous weeks within the farm of interest, and represents *other mobiles* that have *survived* from previous weeks, see details below.
2. λ_{it}^{Adw} is based on counts of adult females in the previous sixteen weeks within the farm of interest, and represents offspring of previous *adult females within* the farm that have *developed* into other mobiles, typically several weeks later, see details below.
3. λ_{it}^{Adn} is based on counts of adult females in the previous sixteen weeks at neighbouring farms, and represents offspring of previous *adult females at neighbouring farms*, see details below.

Details on how each of these terms are modelled are given in the following:

347 *Surviving other mobiles* are modelled as

$$\lambda_{it}^{Os} = \varphi_1^{Os} \cdot y_{i(t-1)}^{Os*} + \varphi_{2it}^{Os} \cdot y_{i(t-2)}^{Os*} \cdot S_{i(t-1)}, \quad (9)$$

348 where:

- 349 • $\varphi_1^{Os} = 1$ is an autoregressive coefficient set to 1 for identifiability.
- 350 • φ_{2it}^{Os} is another autoregressive coefficient that depends on the seawater tem-
 351 perature in the same way as φ_{2it}^{As} in Eq. (6), but with parameters φ_2^{Os*} and
 352 β_2^{Os} .

353 The term representing *adult females within* the farm, whose offspring have *devel-*
 354 *oped* into other mobiles, is modelled as

$$\lambda_{it}^{Adw} = \sum_{l=1}^{l=16} \varphi_{lit}^{Ad} \cdot y_{i(t-l)}^{As*} \cdot n_{i(t-l)}^{\theta^{rep}} / n_{it}^{\theta^{inf}}, \quad (10)$$

355 where

- 356 • $\varphi_{lit}^{Ad}, l = 1, \dots, 16$ are coefficients that vary smoothly by increasing lags,
 357 through the dependency of only three underlying coefficients in the equation

$$\varphi_{lit}^{Ad} = \gamma_{it}^a \cdot [1 - \gamma_{it}^s \cdot (l - \gamma_{it}^c)^2]_+ / c_{it}, l = 1, \dots, 16. \quad (11)$$

358 Here, $[\cdot]_+$ means the non-negative part, γ_{it}^c is the centre in a quadratic curve,
 359 $\gamma_{it}^s > 0$ controls the spread of the curve, γ_{it}^a is its amplitude and c_{it} is a
 360 normalising constant such that the coefficients sum to γ_{it}^a , i.e. $\sum_{l=1}^{l=16} \varphi_{lit}^{Ad} =$
 361 γ_{it}^a . See Figure 4 in Section 3.1 for examples on how the lag structure may
 362 look. The coefficients γ_{it}^s and γ_{it}^a depend on the seawater temperature in

the same way as φ_{1t}^{Od} in Eq. (6), but with parameters $\gamma^{s\bullet}$, β^s and $\gamma^{a\bullet}$, β^a , respectively. Furthermore, γ_{it}^c depends on the seawater temperature as

$$\gamma_{it}^c = 1 - 1/\sqrt{\gamma_{it}^s} + \gamma^{c\bullet} \cdot \exp(\beta^c \cdot (T_{it} - 9)), \quad (12)$$

where $\gamma^{c\bullet}$ and β^c are parameters. This functional form ensures that the minimum development time from eggs to other mobiles increases by decreasing seawater temperatures, see details in the Supplementary Material.

- n_{it} is the number of fish at farm i at time t , measured in million fish, and $n_{i(t-l)}$ is the number of fish l weeks before.
- θ^{rep} and θ^{inf} are non-negative parameters that allow for non-linear dependencies of the numbers of fish at previous lags, i.e. the hosts for reproducing lice at previous lags, and the number of fish that becomes infected by the new lice. Furthermore, θ^{rep} is re-parameterised as

$$\theta^{rep} = \theta^{inf} + \theta^0. \quad (13)$$

If the parameter θ^0 is positive, the infection pressure per fish will increase if the overall number fish increases.

The term representing *adult females* at *neighbouring* farms, whose offspring have *developed* into other mobiles, is modelled as

$$\lambda_{it}^{Adn} = \left(\sum_{j \neq i} \lambda_{ijt}^{Adn} \right)^\delta, \quad (14)$$

where λ_{ijt}^{Adn} is the contribution from the j -th farm given by

$$\lambda_{ijt}^{Adn} = \left(\sum_{l=1}^{l=16} \varphi_{ljt}^{Ad} \cdot y_{j(t-l)}^{A*} \cdot n_{j(t-l)}^{\theta^{rep}} / n_{it}^{\theta^{inf}} \right) \cdot \pi_0 \cdot \exp(\pi_1 \cdot ((d_{ij}^{\pi_2} - 1) / \pi_2)). \quad (15)$$

Here,

- δ is a positive parameter that allows for non-linear dependency of the sum of the contributions from the neighbouring farms. The values of δ and θ^{rep} quantifies the consequences of introducing new neighbouring farms versus increasing the number of fish at the existing neighbouring farms, see the discussion in Section 3.1.
- $n_{j(t-l)}$ is the number of fish at a neighbouring farm j at time $t-l$, i.e. the hosts for reproducing lice.
- π_0 quantifies the importance of neighbouring infection compared to the other sources of infection.
- d_{ij} is the seaway distance between farms i and j .
- π_1 and π_2 are parameters that reflect the effect of the seaway distances to neighbouring farms, and the transformation $(d_{ij}^{\pi_2} - 1) / \pi_2$ is the Box-Cox transformation, which allows for different shapes of the distance function.

2.2.4 Correlations

So far, we have treated the lice counts of adult females (y_{it}^A) and other mobiles (y_{it}^O) at each farm as separate time series. The expected values of one series is modelled as a function of previous values of the other series at the same farm,

and for other mobiles also on the series at neighbouring farms. However, we have not considered potential mutually stochastic dependency within the same week between the various time series of lice counts. It turns out that some of the series are positively correlated (Section 3). It is essential to include such correlations to calculate the correct uncertainty for forecasts more than one step ahead for single time series and even for one step ahead for the average of several time series (Section 2.2.5).

Thus, we need to define a “multivariate zero-inflated negative binomial distribution” (several choices are possible, but none of them are the single obvious one), and we need to select a suitable model structure. Our approach is to start with a multivariate standard normal distribution with a given correlation structure, consisting of q correlated univariate standard normal variables $z_j, j = 1, \dots, q$ (one for each farm). Then each univariate standard normal variable z (dropping the farm index for a while) is transformed to a zero-inflated negative binomial variable with a given set of parameters μ, p^z and ν (who depend on the farm and the time point). This procedure induces a correlation structure at the zero-inflated negative binomial scale. The transformation can be divided into two steps: First, z is transformed to a uniform variable u by $u = \Phi(z)$, where Φ is the cumulative distribution function for a standard normal variable. In the next step, u is transformed to a zero-inflated negative binomial variable y by $y = F_{\mu, p^z, \nu}^{-1}(u)$, where $F_{\mu, p^z, \nu}^{-1}$ is the inverse cumulative distribution function for a zero-inflated negative binomial variable with the given set of parameters. These two steps can be condensed to $y = F_{\mu, p^z, \nu}^{-1}(u) = F_{\mu, p^z, \nu}^{-1}(\Phi(z))$.

We consider four types of pairwise correlations; i) between adult females and other mobiles within farms, and ii) between adult females, iii) between other

mobiles and iv) between adult females and other mobiles at different farms. Let $\rho_{ij}^{s,s'}$ denote the correlation at the standard normal scale between transformed lice counts at stages s and s' at farms i and j . We expect that correlations between farms i and j depend on the their corresponding seaway distances d_{ij} , but assume that between farm correlations are exact 0 for seaway distances larger than 100 km. Our correlation model at the standard normal scale are then

$$\rho_{ii}^{wAO} = \rho^{wAO}, \quad (16)$$

$$\rho_{ij}^{bAA} = \rho^{bAA\bullet} \cdot \exp(\beta_1^{bAA} d_{ij}) \text{ for } i \neq j \text{ and } d_{ij} < 100 \text{ km}, \quad (17)$$

$$\rho_{ij}^{bOO} = \rho^{bOO\bullet} \cdot \exp(\beta_1^{bOO} d_{ij}) \text{ for } i \neq j \text{ and } d_{ij} < 100 \text{ km}, \quad (18)$$

$$\rho_{ij}^{bAO} = \rho^{bAO\bullet} \cdot \exp(\beta_1^{bAO} d_{ij}) \text{ for } i \neq j \text{ and } d_{ij} < 100 \text{ km}, \quad (19)$$

where the ρ 's and β 's are parameters to be estimated. The parameters $\rho^{bAA\bullet}$, $\rho^{bOO\bullet}$ and $\rho^{bAO\bullet}$ are interpreted as correlations between farms with seaway distances exactly 0, but in practice there are usually at least 1-2 km between farms. For estimating these parameters, we follow the opposite procedure, i.e. we transform from the observed zero-inflated negative binomial variables to standard normal variables, and then estimate the correlation parameters. If an observation y was sampled from a continuous variable with cumulative distribution function $F(y)$, the transformation to the standard normal scale would be unique by $z = \Phi^{-1}(F(y))$. However, since y is discrete, the transformation of y to u on the 0-1 scale is only determined up to an interval, and all values of u within this interval would give the same y . We handle this by simulating a value u^{sim} uniformly within this interval, i.e. $u^{sim} \sim Uniform(p_1, p_2)$, where $p_1 = P(Y \leq y - 1) = F_{\mu,p^z,\nu}(y - 1)$ and $p_2 = P(Y \leq y) = F_{\mu,p^z,\nu}(y)$, and then $z = \Phi^{-1}(u^{sim})$. Here, $P(\cdot)$ means probability, Y is a stochastic variable and y

442 a possible observed value. Each observed lice count is transformed separately in
443 this way.

444 After transforming all observations to the standard normal scale, we calculate
445 pairwise empirical correlations $r_{ij}^{s,s'}$ between all variables (time series) that overlap
446 in time. Then, the parameters are estimated by the least squares fits of the three
447 variants of the non-linear regression equations $r_{ij}^{ss'} = \exp(\beta_0^{bss'} + \beta_1^{bss'} d_{ij}) + \varepsilon_{ij}$
448 where ε_{ij} is random noise, and of the simpler variant $r_{ii}^{wAO} = \exp(\beta_0^{wAO}) + \varepsilon_{ii}$ for
449 the within farm correlations. This is a Gaussian model with a logarithmic link
450 function and standard software for generalised linear models may be therefore
451 be used. The estimates of ρ parameters of the right sides of Eqs. (16)-(19) are
452 then given by back-transformations of the form $\hat{\rho}^{wAO} = \exp(\hat{\beta}_0^{wAO})$ and $\hat{\rho}^{bss'\bullet} =$
453 $\exp(\hat{\beta}_0^{bss'})$.

454 Since each variable is transformed independently of the others, the simulation
455 step eliminates some of the correlation structure, resulting in biased parameter
456 estimates giving too low correlations. To adjust for this we apply bias correction
457 by the following parametric bootstrap procedure:

- 458 1. Estimate the β parameters by the regression procedure above and denote
459 the estimates by $\tilde{\beta}$.
- 460 2. Simulate a data set from the estimated model on the zero-inflated negative
461 binomial scale with the same size as the observed data.
- 462 3. Transform the simulated observations to the standard normal scale and
463 estimate the parameters, denoting them by $\tilde{\beta}^b$.
- 464 4. Repeat 1-3 for $b = 1, \dots, B = 20$, and compute the average of each parameter
465 estimate as $\tilde{\beta}^* = 1/B \sum_b \tilde{\beta}^b$.

466 5. The final estimate is then given by $\hat{\beta} = 2\tilde{\beta} - \tilde{\beta}^*$. This standard bootstrap
 467 bias correction formula (Efron and Tibshirani, 1993, see e.g.) is based on
 468 the assumption that $(\tilde{\beta} - \beta)$ has approximately the same distribution as
 469 $(\tilde{\beta}^b - \tilde{\beta})$, where β is the true parameter value.

470 For investigating the correlations between the original lice counts y_{it} ($i = 1, 2, \dots$)
 471 in the same week t , with corresponding parameters μ_{it} , p_{it}^z and ν_{it} , we consider the
 472 Pearson residuals $(y_{it} - \mu_{it})/s_{it}$, where $s_{it} = \sqrt{n\mu_{it} + [(n^2\mu_{it}^2)/(1 - p_{it}^z)](1/\nu_{it} + p_{it}^z)}$
 473 is the standard deviation of y_{it} , see the Supplementary Material. After substitut-
 474 ing the parameter values by their estimates, we calculate empirical correlations
 475 between all pairs of residual series. We summarise the correlations by regressing
 476 them on the corresponding seaway distances with the same structure as Eqs. (16)-
 477 (19). We compare this empirical correlation structure with the corresponding
 478 structure in data simulated from the model, to ensure that our model is able to
 479 reconstruct the correlation structure in the observed data.

480 2.2.5 Forecasts

481 For forecasting ahead in time, we use the following procedure:

- 482 1. With observations up to and including time t , calculate μ_{t+1} , p_{t+1}^z and ν_{t+1}
 483 for all time series.
- 484 2. Simulate multivariate normal variables with correlations given from Eqs. (16)-
 485 (19).
- 486 3. Transform the standard normal variables to zero-inflated negative binomial
 487 variables, using the parameters calculated in 1.

- 488 4. Go one step ahead to time $t + 1$ and let the simulated zero-inflated negative
489 binomial variables from 3 take the role as real observations.
- 490 5. Repeat 1-4 until the maximum forecast horizon.
- 491 6. Repeat 1-5 $nsim = 200$ times
- 492 7. Take the average of all simulations as the point forecast and calculate the
493 95% prediction interval as the 2.5 and the 97.5 quantiles of the simulated
494 values. This is done for adult females and other mobiles at each farm and
495 for the sum over farms.

496 2.2.6 Estimation

497 The various models were estimated by fitting them to observed lice counts be-
498 tween week 17 in 2012 until week 44 in 2016, whereas data from the first sixteen
499 weeks in 2012 were used to construct lagged variables. The models for adult
500 females and other mobiles were estimated by maximizing the log likelihood (see
501 Supplementary material for the likelihood expression) using the function *optim*
502 in the statistical software R, using the method of Byrd et al. (1995). Parameter
503 uncertainties were based on the observed Fisher information matrix (Pawitan,
504 2001) and are reported as 95% Wald confidence intervals. Some parameters
505 were estimated on the logit or the logarithmic scale and transformed back to the
506 original scale used in the model descriptions, giving non-symmetrical confidence
507 intervals on the original scale. The correlation models were estimated using the
508 *glm* function in R.

3 Results and discussion

3.1 Estimated models for expected lice abundance

The estimated parameters with 95% confidence intervals for the expected abundances are given in Tables 2 and 3. The estimates for the corresponding submodels for the excess zero probabilities p^z and the aggregation parameters ν are found in the Supplementary materials. Below, we first illustrate the results by figures and then comment on the parameters that are not covered by these figures.

Figure 1 shows time plots of the expected abundance of lice and the corresponding observed lice abundance averaged over all farms and for two selected farms. The expected abundance of adult females (panel A) and other mobiles (panel B), along with the proportional contribution of the various additive sources of infections (panels C,D), are shown for a small area in the South West of Norway in week 44 in 2013 in Figure 2. In panel C, the proportions are based on Eq. (2), and for instance the contributions from surviving adult females are calculated as $\lambda_{it}^{As} / (\lambda_{it}^{As} + \lambda_{it}^{Od} + \lambda_{it}^{int})$. In panel D, the proportions are based on Eq. (8), and are calculated similarly.

Figure 3 shows the estimated lag structure in the model for adult females at various seawater temperatures. When the temperature increases, the first order lag becomes increasingly more important than the second order lag, and the importance of the development from other mobiles to adult females increases compared to the surviving adult females. Both these effects are explained by the well-known fact that the rate of development from one stage to the next increases by increasing seawater temperature. When the seawater temperature is 4 °C, φ_{2it}^{Od} is larger than φ_{1it}^{Od} (upper right panel), which suggests that the model could be

improved by including a third lag. However, it turns out that the improvement is not significant, so we keep only two lags in the final model.

Figure 4 corresponds to Figure 3, but shows the lag structure for the other mobiles model. Again, the increasing development rates by increasing temperature explain the different patterns in the panels. The lag structure for the development from adult females to the next generation other mobiles is centred around 10 days at 4°C, 6 days at 9°C and 4 days at 14°C (Figure 4, right panels). These time delays are comparable with some previous studies. Stien et al. (2005) presented a population model for salmon lice with equations for *minimum* development times for each stage to the next, where the estimated parameters were based on a synthesis of laboratory experiments. Their model did not include the time it takes for an infective copepodid to infect a fish host, but if we assume that this takes 4 days, corresponding to the expected lifetime of the copepodids (1/daily mortality, Stien et al. (2005)), the sum of the minimum development times over all relevant stages from eggs to pre-adults, amount to 11.3, 5.3 and 3.2 weeks for seawater temperatures 4, 9 and 14°C, respectively. A more detailed population model estimated on full scale production data from 32 Norwegian salmon farms, was developed by Aldrin et al. (2017). This study presented estimates for the *median* development times for each stage, and the sum of these amount to 12.0, 5.7 and 4.3 weeks for seawater temperatures 4, 9 and 14°C, respectively. A third comparison can be made by combining results from two recent laboratory studies (Eichner et al., 2015; Samsing et al., 2016). If we still assume that it takes 4 days for a copepodid to infect a fish host and one day more before it develops to the chalimus stage, their results indicate that it takes 3.5-4.1 weeks to develop from eggs to pre-adults at 10°C.

Now, we continue by commenting on the effect of explanatory variables included in the factors κ_{it}^{usc} in Eqs. (2) and (8), i.e. time, seawater temperature, latitude and fish weight. The various effects are presented as relative effects compared to a reference value, i.e. as $\exp(\hat{\beta}x)/\exp(\hat{\beta}x^{ref})$ if we consider an explanatory variable x with reference value x^{ref} and estimated regression coefficient $\hat{\beta}$.

Everything else unchanged, the expected lice abundances decrease over time for both adult females and other mobiles (Figure 5). One plausible explanation for this is that lice control practices have changed during the data period. In 2012, all lice treatments were medical treatments. However, as medical treatments have shown reduced effects due to louse resistance (Aaen et al., 2015; Jansen et al., 2016), new methods to shield farms from infection and non-medical treatments are increasingly being applied. These are not accounted for in our model due to the lack of sufficient data.

Figure 6 shows the relative effects of seawater temperatures at two different latitudes. For both adult females and other mobiles, the relative effect increases with increasing temperatures for low and medium temperatures. For temperatures above 11-12°C, however, the relative effect tends to decrease again for other mobiles. Furthermore, the effect of temperature difference between weeks t and $t - 1$ is similar in the two models, with slightly lower relative effect in periods with increasing seawater temperatures (spring and summer). In contrast, the latitude has opposite effects in the two models. For adult females the relative effect increases with latitude, whereas for other mobiles it decreases (remember that this is conditional on temperatures and everything else being equal).

The mean fish weight at susceptible farms is also an important explanatory variable. The relative effect increases with increasing weight of the fish (Figure 7).

For other mobiles, one plausible explanation may be that the increasing surface of the fish facilitates host finding and the infection process for the parasite, as has repeatedly been suggested previously (Jansen et al., 2012; Aldrin et al., 2013). However, this does not explain the even more pronounced effect of fish weight for adult females, since they recruit from other mobiles and not through an infection process. Demographic processes that could contribute to the observed effect of fish weight on adult female lice could either be fish size dependent survival or recruitment of the adult females. Although speculative, we suggest that adult female mortality may be high on small fish due to the extensive use of cleaner fish while the farmed salmon are relatively small. With regard to recruitment from other mobiles, we suspect that this may be under-estimated for large fish. Other mobile lice are comparably small of size and easy to oversee under standard counting procedures and under-reporting related to fish size has also been suggested earlier (Aldrin et al., 2013).

The relative effect of infection pressure from neighbouring farms decreases (only relevant for other mobiles) rapidly by increasing seaway distances to the neighbours (Figure 8). Furthermore, the infection pressure from a neighbouring farm infinitesimally close is lower than the internal infection pressure within a farm. Interestingly, the form of the function in Figure 8 resembles the relative lice abundances in Figures 3 and 4 in Salama et al. (2016), obtained from simulating the spread of salmon lice in Loch Linnhe using a hydrodynamic model and particle tracking.

We end this subsection by commenting on the remaining parameter estimates in Tables 2 and 3. The estimated treatment mortalities are almost equal in the two models, being 44% for adult females and 47% for other mobiles. This seems to be

very low. However, the estimated treatment effects include all the various medical treatments and it is not clear in the data whether a given treatment covers all or only parts of the farm cages. This implies that lice counts post treatment may in some cases be from non-treated cages leading to underestimated treatment effects. The estimated values of the α parameters, which allow for non-linear dependency of previous weeks lice counts, are also very similar (0.874 and 0.889). The estimated value of the intercept λ_{it}^{int} in Eq.(2) for adult females is small (λ^{int} is small compared to 1) and decreases by increasing seawater temperatures ($\beta^{int} < 0$). The intercept is small also for other mobiles, but the estimate of β^{int} for this model is close to 0 and non-significant. The parameter θ^0 is estimated to be positive, which means that the infection pressure per fish will increase if the number fish increases in general, i.e. if the number of fish increases by the same factor for both a susceptible farm and its infective neighbours. The estimate of the exponent $\theta^{rep} = \theta^{inf} + \theta^0$ in Eq.(13) is $0.391 + 0.171 = 0.562$, and the estimate of the exponent δ in Eq.(15) is 0.709. This means that if the numbers of fish are doubled at all neighbouring farms, the infection pressure for the susceptible farm will increase by 32% ($(2^{0.562})^{0.709} = 1.32$), as long as the lice abundance at the neighbouring farms as well as the number of fish at the susceptible farm are held constant. On the other hand, if the number of neighbouring farms are doubled, but with unchanged seaway distances to the susceptible farm, the infection pressure will increase by 63% ($2^{0.709} = 1.63$). We have no explanation for the asymmetric result of increasing the number of fish at the neighbouring farms compared to increasing the number of neighbouring farms. However, symmetry may be achieved by setting $\theta^{rep} = 1$, i.e. $\theta^0 = 1 - \theta^{inf}$. For a model with this restriction, the infection pressure will increase by 62% both by doubling the number of fish at the neighbours and by doubling the number of

neighbours. However, this model gave a significantly (p value ≈ 0) worse fit to the data, decreasing the log likelihood by 107. Therefore, by the configuration of farms in the present data set, an analytic result suggests that comparably few farms with many fish and large between farms distances is effective in terms of minimising the output of salmon lice. One should, however, be careful to interpret this as a causal effect, since there are many potential confounding factors related to farm size, for instance how the farms are managed or in which regions they are located.

If a farm is active in week t , but not in the previous week, the fish cohort at the farm is considered as stocked if the mean fish weight is less than 250 g and relocated otherwise. This is modelled by including a corresponding indicator variable in the expression for κ_{it}^{susc} in Eq.(3). Remember that previous lice counts in this case by our definition is 0. If a fish cohort is stocked, its expected abundance of adult females is reduced by 86% (since $1 - \exp(-2.002) = 0.86$) compared to a farm that was active in the previous week, but with no observed lice. The corresponding reduction for other mobiles is 76%. On the other hand, if a fish cohort is relocated, the comparable expected lice abundance the first week after relocation is a factor 5.2 ($\exp(1.653) = 5.2$) for adult females and 3.5 for other mobiles higher than in an active farm without observed lice the previous week. This is probably because relocated fish bring lice with them from their previous farm.

Concerning the zero-inflation part of the model, the probabilities for excess zero lice counts, compared to a pure negative exponential distribution, are negligible in situations with positive lice counts the previous week. However, if there either was zero lice counts the previous week or if the farm were not active last week,

the probabilities for excess zeroes are high and in the range 0.25-0.6 (Figure 1 in the Supplementary material).

Table 2: Estimated parameters in the model for expected abundance μ_{it} of adult females with 95% confidence intervals for the selected model.

Parameter group	Variable name or parameter description	Parameter symbol	Est.	Lower	Upper	Trans.
$\lambda_{it}^{As}, \lambda_{it}^{Od}$	Non-linear dependency of counts	α	0.874	0.866	0.882	
λ_{it}^{As}	AR-coefficient, lag 1	φ_1^{As}	1	Fixed		
λ_{it}^{As}	Value of φ_{2it}^{As} when $T_{it} = 9$	$\varphi_2^{As\bullet}$	0.314	0.294	0.336	log
λ_{it}^{As}	Temperature dependency of φ_{2it}^{As}	β_2^{As}	-0.063	-0.081	-0.045	
λ_{it}^{Od}	Value of φ_{1it}^{Od} when $T_{it} = 9$	$\varphi_1^{Od\bullet}$	0.107	0.100	0.114	log
λ_{it}^{Od}	Temperature dependency of φ_{1it}^{Od}	β_1^{Od}	0.064	0.049	0.079	
λ_{it}^{Od}	Intercept in φ_{2it}^{Od}	$\varphi_2^{Od\bullet}$	0.055	0.051	0.060	log
λ_{it}^{Od}	Temperature dependency of φ_{2it}^{Od}	β_2^{Od}	-0.080	-0.103	-0.058	
λ_{it}^{int}	Value of λ_{it}^{int} when $T_{it} = 9$	$\lambda^{int\bullet}$	0.014	0.013	0.015	log
λ_{it}^{int}	Temperature dependency of λ_{it}^{int}	β^{int}	-0.057	-0.068	-0.046	
susceptibility κ_{it}^{susc}	Reference value of κ_{it}^{susc}	$\kappa^{susc\bullet}$	0.480	0.468	0.492	log
" - "	(time-week 30 2014)*	β_k^{susc}	-0.026	-0.031	-0.021	
" - "	(temp-9)*	" - "	0.040	0.034	0.045	
" - "	(temp-9) ² *	" - "	-0.0024	-0.0029	-0.0018	
" - "	temp _t - temp _{t-1} *	" - "	-0.028	-0.035	-0.022	
" - "	(latitude-64)*	" - "	0.023	0.021	0.025	
" - "	log(weight)-log(2)*	" - "	0.246	0.238	0.255	
" - "	1 if stocked in week t, 0 otherwise	" - "	-2.002	-6.258	2.253	
" - "	1 if relocated in week t, 0 otherwise	" - "	1.653	0.961	2.346	
treatment κ_{it}^{treat}	treatment mortality	θ^{tm}	0.439	0.424	0.455	logit

* Seawater temperature is measured in °C, latitude in °N, weight in kg and time in years

Est.: Estimate

Lower: Lower bound of 95% confidence interval

Upper: Upper bound of 95% confidence interval

Trans: Transformation used in optimisation

Table 3: Estimated parameters in the the model for expected abundance μ_{it} of other mobiles with 95% confidence intervals for the selected model.

Parameter group	Variable name or parameter description	Parameter symbol	Est.	Lower	Upper	Trans.
λ_{it}^{Adn}	Non-linear dependency of infection from neighbours	δ	0.709	0.676	0.741	
$\lambda_{it}^{Os}, \lambda_{it}^{Adw}, \lambda_{it}^{Adn}$	Non-linear dependency of counts	α	0.889	0.883	0.896	
λ_{it}^{Os}	AR-coefficient, lag 1	φ_1^{Os}	1	Fixed		
λ_{it}^{Os}	Value of φ_{2it}^{Os} when $T_{it} = 9$	$\varphi_2^{Os\bullet}$	0.157	0.148	0.168	
λ_{it}^{Os}	Temperature dependency of φ_{2it}^{Os}	β_2^{Os}	-0.130	-0.151	-0.109	
$\lambda_{it}^{Adw}, \lambda_{it}^{Adn}$	Amplitude of lag curve when $T_{it} = 9$	$\gamma^{a\bullet}$	0.262	0.243	0.283	log
$\lambda_{it}^{Adw}, \lambda_{it}^{Adn}$	Temperature dependency of amplitude	β^a	0.165	0.153	0.177	
$\lambda_{it}^{Adw}, \lambda_{it}^{Adn}$	Constant in centre of lag curve when $T_{it} = 9$	$\gamma^{c\bullet}$	7.445	7.322	7.570	log
$\lambda_{it}^{Adw}, \lambda_{it}^{Adn}$	Temperature dependency of centre	β^c	-0.118	-0.122	-0.114	
$\lambda_{it}^{Adw}, \lambda_{it}^{Adn}$	Spread of lag curve when $T_{it} = 9$	$\gamma^{s\bullet}$	0.165	**		log
$\lambda_{it}^{Adw}, \lambda_{it}^{Adn}$	Temperature dependency of spread	β^s	0.217	0.216	0.219	
$\lambda_{it}^{Adw}, \lambda_{it}^{Adn}$	Non-linear dependency of no. fish	θ^{inf}	0.391	0.356	0.427	
$\lambda_{it}^{Adw}, \lambda_{it}^{Adn}$	Non-linear dependency of no. fish	θ^0	0.171	0.129	0.213	
λ_{it}^{Adn}	Relative importance of neighbouring infection	π_0	0.503	0.426	0.595	log
λ_{it}^{Adn}	Parameter in Box-Cox transformation	π_1	-0.374	-0.313	-0.436	
λ_{it}^{Adn}	Parameter in Box-Cox transformation	π_2	0.692	0.620	0.764	
λ_{it}^{int}	Value of λ_{it}^{int} when $T_{it} = 9$	$\lambda^{int\bullet}$	0.018	0.016	0.020	log
λ_{it}^{int}	Temperature dependency of λ_{it}^{int}	β^{int}	0.0045	-0.0083	0.0173	
susceptibility κ_{it}^{susc}	Reference value of κ_{it}^{susc}	$\kappa^{susc\bullet}$	0.908	0.896	0.920	
-"	(time-week 30 2014)*	β_k^{susc}	-0.039	-0.043	-0.035	
-"	(temp-9)*	-"	0.033	0.029	0.037	
-"	(temp-9) ² *	-"	-0.0078	-0.0083	-0.0073	
-"	temp _t - temp _{t-1} *	-"	-0.034	-0.040	-0.028	
-"	(latitude-64)*	-"	-0.014	-0.016	-0.013	
-"	log(weight)-log(2)*	-"	0.103	0.096	0.110	
-"	1 if stocked in week t, 0 otherwise	-"	-1.429	-2.129	-0.729	
-"	1 if relocated in week t, 0 otherwise	-"	1.259	0.815	1.703	
treatment κ_{it}^{treat}	treatment mortality	θ^{tm}	0.469	0.456	0.482	logit

* Seawater temperature is measured in °C, latitude in °N, weight in kg and time i year

** Confidence limits not available due to unknown standard error. The optimisation routine were not able to compute the standard errors for these coefficients, probably due to to high correlations which give numerical instabilities while computing the Hessian matrix.

Est.: Estimate

Lower: Lower bound of 95% confidence interval

Upper: Upper bound of 95% confidence interval

Trans: Transformation used in optimisation

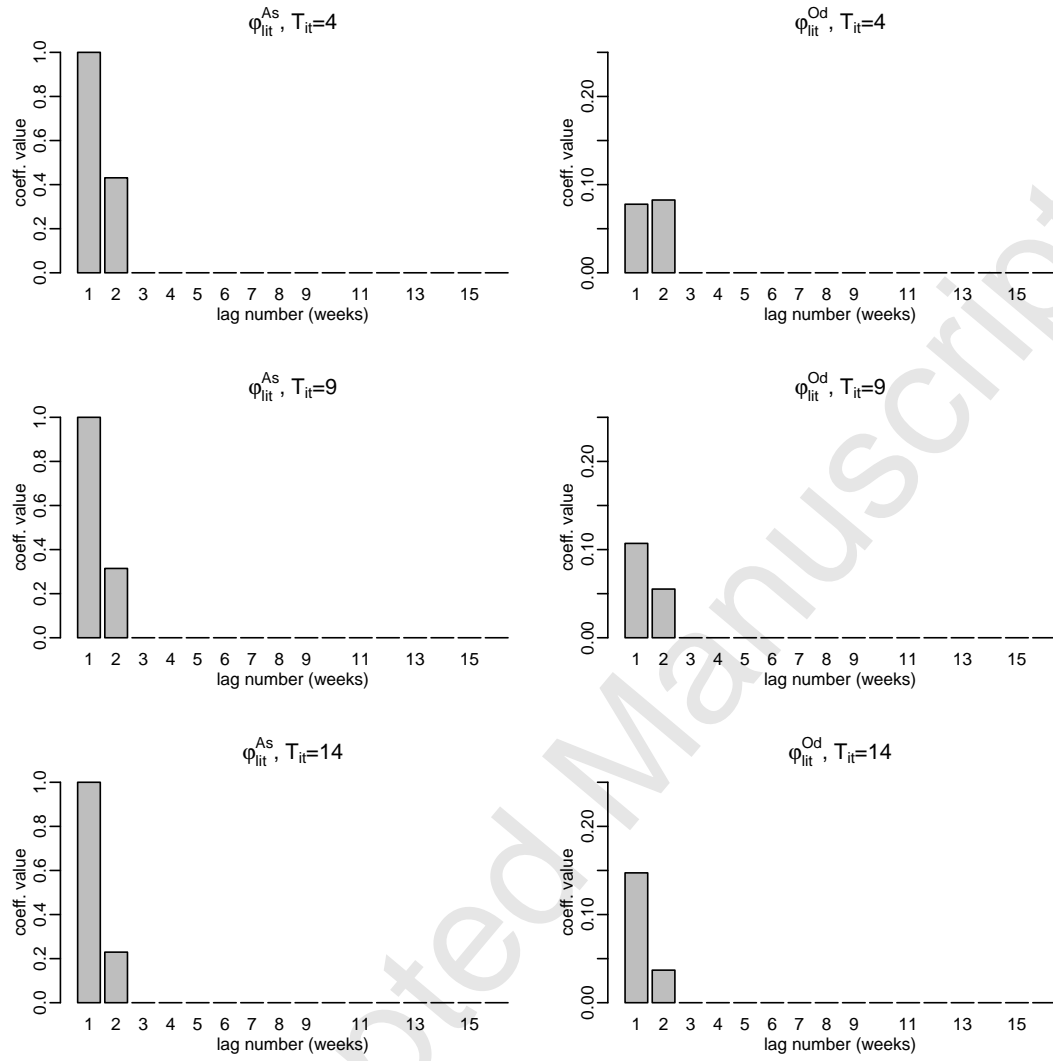


Figure 3: Autocorrelation coefficients in the A model, for λ_{it}^{As} (left panels) and λ_{it}^{Od} (right panels) and for seawater temperatures 4, 9 and 14°C (upper, mid and lower panels, respectively).

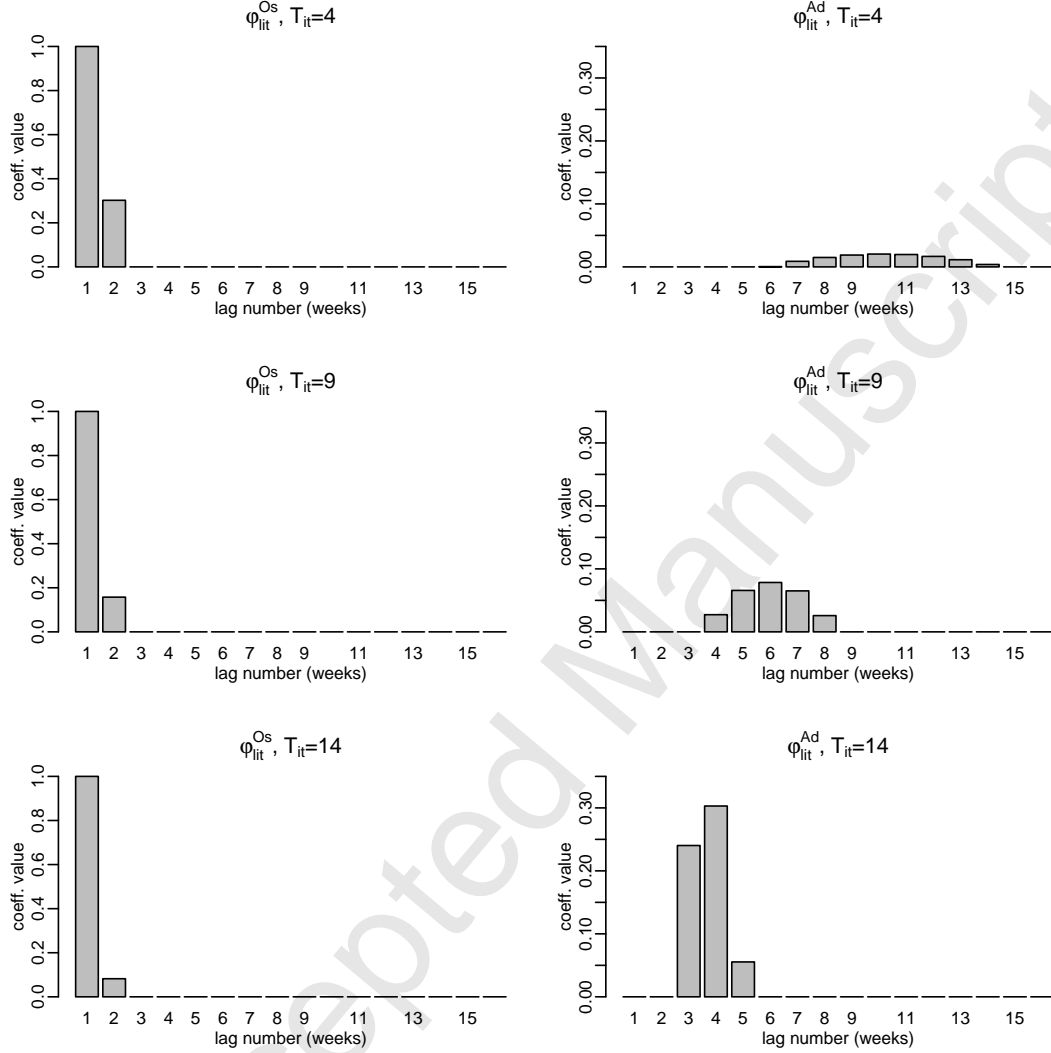


Figure 4: Autocorrelation coefficients in the O model, for λ_{it}^{Os} (left panels) and λ_{it}^{Adw} (right panels) and for seawater temperatures 4, 9 and 14°C (upper, mid and lower panels, respectively). The lag structure for infection from the previous generation adult females at a neighbouring farm (λ_{it}^{Adn} , not shown) is similar to the lag structure for infection from the previous generation adult females within the farm (λ_{it}^{Adw}), but it is first multiplied by a factor that depends on the seaway distance to the neighbour through $\pi_0 \cdot \exp(\pi_1 \cdot ((d_{ij}^{\pi_2} - 1)/\pi_2))$, and then raised to the power of δ , see Eqs. (15) and (14).

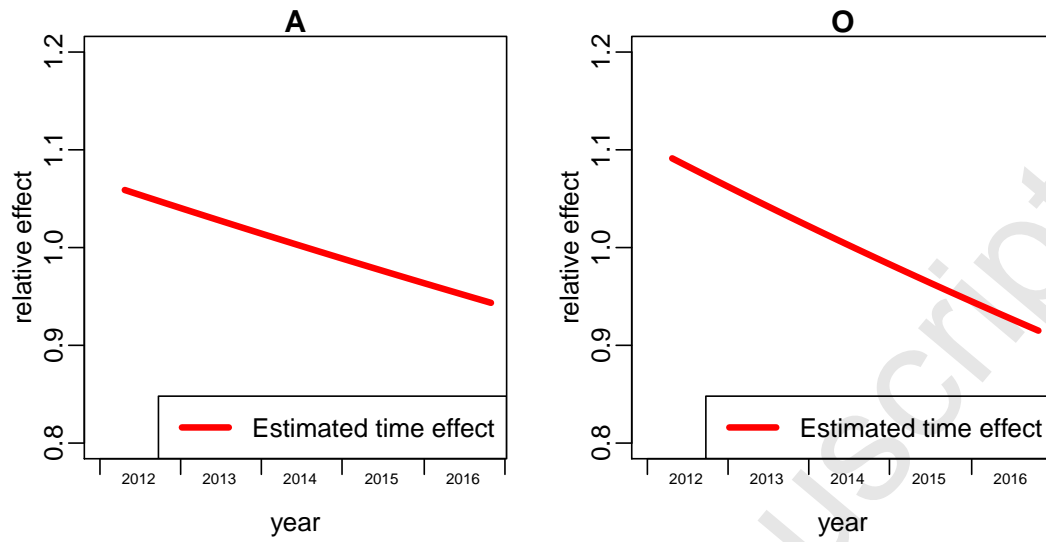


Figure 5: Relative effects of time the A and O models, with the effects set to 1 at week 30 2014.

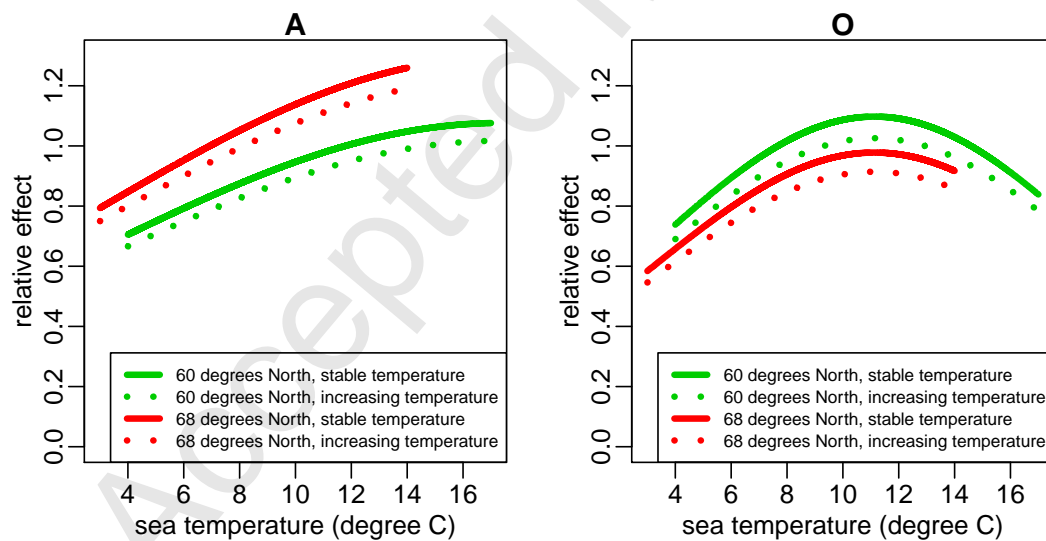


Figure 6: Relative effects of seawater temperatures and latitude in the A and O models, with the effects set to 1 for a constant seawater temperature 9°C at 64°N. The solid curves show the effects when the temperatures in the current and the previous week are equal, whereas the dotted curves show the effects when the temperature is increased by 2°C from the previous to the current week.

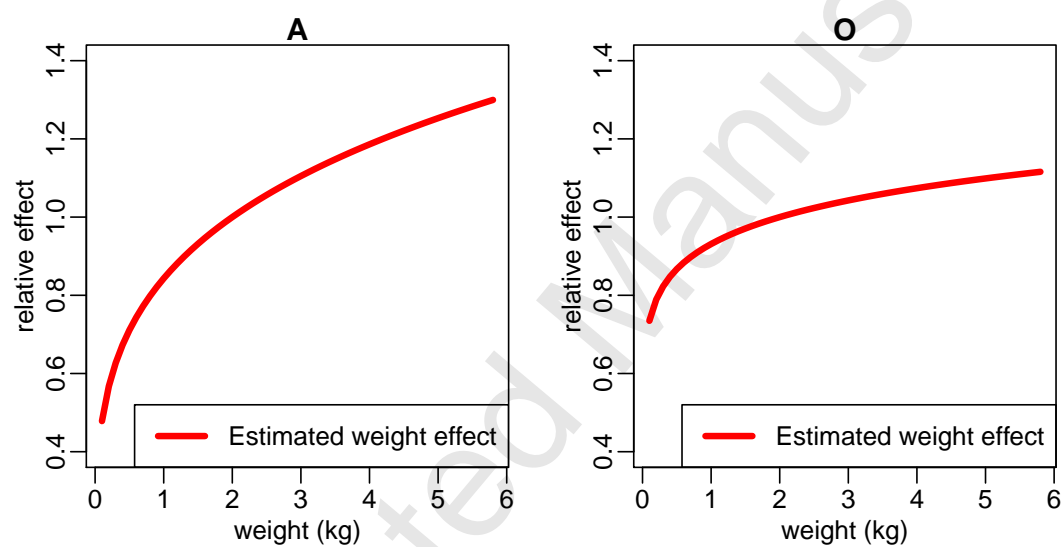


Figure 7: Relative effects of fish weight in the A and O models, with the effects set to 1 for fish at 2 kg.

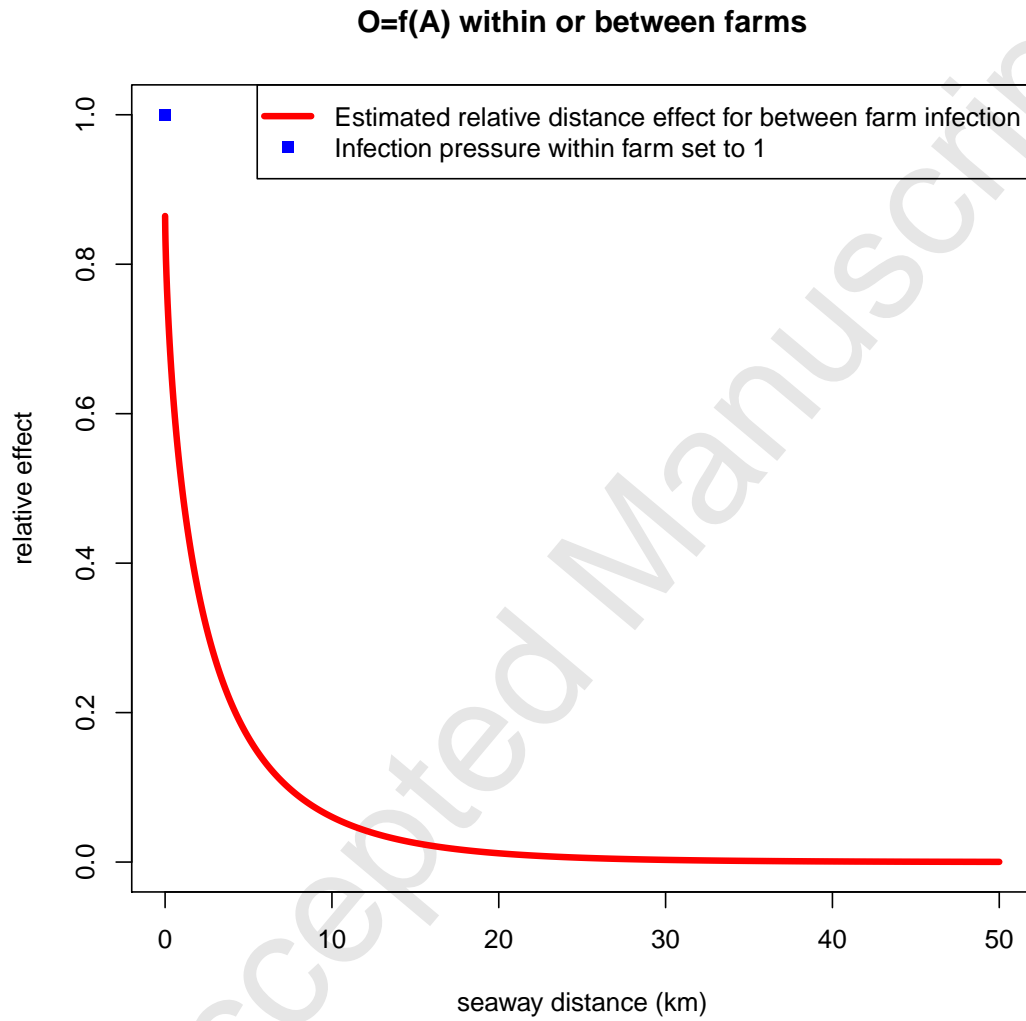


Figure 8: Relative effect of seaway distance for infection from neighbouring farms in the O model, where the within farm infection is the reference point set to 1. The relative effect is defined as the expression $\pi_0 \cdot \exp(\pi_1 \cdot ((d_{ij}^{\pi_2} - 1)/\pi_2))$ from Eq. (15).

3.2 The correlation model

The estimated correlation parameters are given in Table 4. The estimated model parameters defined in Eqs. (17)-(19) are given in the leftmost columns. The β_1 parameters are negative, which means that the correlations decrease by increasing seaway distances between farms. The bias corrected parameters, which have been used in the final model, imply higher correlations than the ordinary ones, with higher values of ρ (correlations at zero distances) and lower or equal values of β_1 . The induced correlations on the original scale are given in the rightmost columns, and we see that the induced correlations from the bias corrected model parameters match the observed correlations well.

Table 4: Estimated correlation parameters.

Correlation type	Standard normal scale				Lice count scale					
	Ordinary		Bias corrected		Empirical		Ordinary		Bias corrected	
	ρ	β_1	ρ	β_1	ρ	β_1	ρ	β_1	ρ	β_1
wAO	0.347		0.484		0.375		0.268		0.339	
bAA	0.069	-0.036	0.107	-0.034	0.107	-0.057	0.045	-0.036	0.072	-0.031
bOO	0.138	-0.024	0.158	-0.024	0.159	-0.028	0.118	-0.025	0.131	-0.027
bAO	0.045	-0.027	0.060	-0.027	0.044	-0.026	0.040	-0.034	0.040	-0.029

3.3 Predictions

To illustrate how the model can be used for prediction, we re-estimated the model without the data for the last eight weeks (weeks 37-44 in 2016), and made predictions 1-8 weeks ahead using lice counts up to and including week 36 in 2016. Figure 9 shows the predictions with 95% prediction limits in average over all farms and for the same two farms as was shown in Figure 1. Here, these predictions are conditioned on the observed seawater temperatures as well as the lice

678 treatments in the prediction period. In practice, one has to predict the seawater
679 temperatures as well, but this should be quite easy, since the temperatures are
680 rather predictable by season. Regarding lice treatments, one could compute pre-
681 dictions both with and without treatments, and use these predictions as a guide
682 to whether one should treat or not during the next weeks to avoid lice abundance
683 becoming too high.

684 The predictions for the average lice abundances (left panels in Figure 9) tend to
685 be too high at the end of the prediction period, for both adult females and other
686 mobiles. One reason for this is probably that the predictions are conditioned on
687 the true lice treatments ahead in time. In real life, high abundances of lice induce
688 treatments. In the simulations, however, the true lice treatments may occur when
689 lice abundances by chance are rather low. Treatment on comparatively lower lice
690 abundance will reduce the total effect of treatments in the simulations compared
691 to the real data.

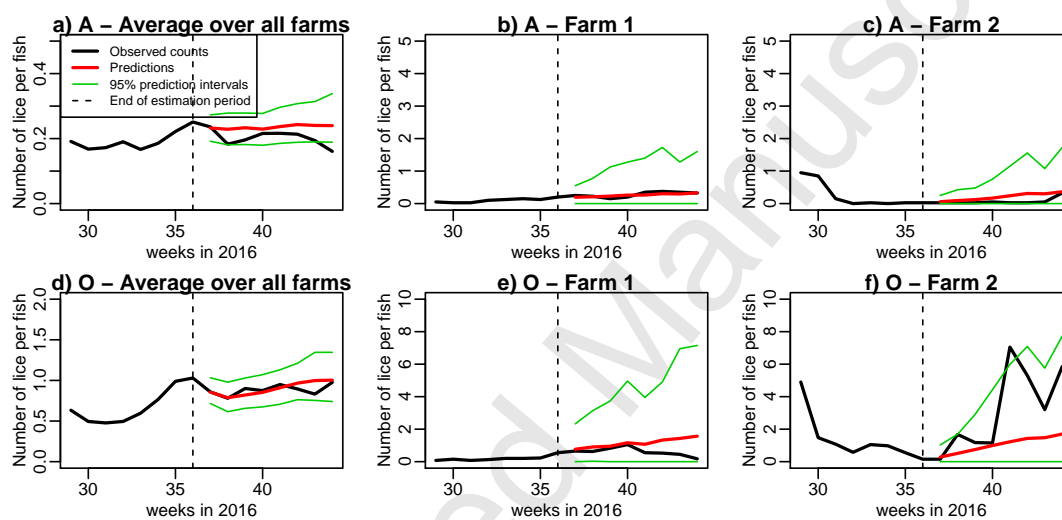


Figure 9: Observed (black) and predicted (red) lice abundance of adult females (upper panels) and other mobiles (lower panels) in average over all farms (panels a and d), and for two separate farms (panels b, c, e and f). The predictions for weeks 37-44 2016, with corresponding 95% prediction intervals (green), are based on lice counts up to week 36 2016.

692 3.4 Conclusions

693 The present paper presents a model for salmon lice abundance covering all marine
 694 salmon farms along the Norwegian coast. Fitting the model to weekly data over
 695 a five year period reveals biologically relevant characteristics of the salmon host-
 696 salmon louse parasite association in salmon farming. The model will be used
 697 as a simulation tool to explore large-scale effects of various salmon louse control
 698 strategies.

699 Several refinements of the present model can be suggested. Salinity is known
 700 to affect salmon lice abundance but is not a part of the model at present, since
 701 salinity measurements on farms are not available. However, salinity calculated by
 702 hydrodynamic models has now become available for the whole coast of Norway,
 703 and may be included as an extra variable in the κ^{sus} term.

704 In our model, we have used the seaway distance d_{ij} as the distance measure be-
 705 tween two farms i and j . However, without any change in the model, this may be
 706 replaced by a “sea current distance” c_{ij} , i.e. an index of average contact between
 707 farms calculated by simulating the spread of sea lice larvae from a hydrodynamic
 708 model. This allows for non-symmetrical distances, i.e. the contact c_{ij} from farm
 709 j to i may differ from the contact c_{ji} in the opposite direction. However, the use
 710 of such distances require that they are calculated for all pairs of farms covered
 711 by the model and over the time covered by the model since the hydrodynamic
 712 forcing will change over time. At present, such data are not available.

713 Acknowledgements

714 This work was funded by the Research Council of Norway through the project:
 715 254830/E40 “Host density and pathogen transmission in salmon aquaculture: ef-
 716 fects of increased production and pathogen control policies”. In addition, Henrik
 717 Stryhn was supported by The Research Council of Norway with a personal grant
 718 (Project: 268051/E40 “Stochastic models on pathogen transmission in aquacul-
 719 ture”).

720 References

- 721 Aaen SM, Helgesen KO, Bakke MJ, Kaur K, Horsberg TE. 2015. Drug resistance
 722 in sea lice: a threat to salmonid aquaculture. *Trends in Parasitology* **31**: 72–81,
 723 doi:10.1016/j.pt.2014.12.006.
- 724 Abolofia J, Asche F, Wilen JE. 2017. The Cost of Lice: Quantifying the Impacts
 725 of Parasitic Sea Lice on Farmed Salmon. *Marine Resource Economics* **32**: 329–
 726 349, doi:10.1086/691981.
- 727 Aldrin M, Huseby RB, Stien A, Grøntvedt RN, Viljugrein H, Jansen PA. 2017.
 728 A stage-structured Bayesian hierarchical model for salmon lice populations at
 729 individual salmon farms - Estimated from multiple farm data sets. *Ecological*
 730 *Modelling* **359**: 333–348, doi:10.1016/j.ecolmodel.2017.05.019.
- 731 Aldrin M, Storvik B, Kristoffersen AB, Jansen PA. 2013. Space-time modelling of
 732 the spread of salmon lice between and within Norwegian marine salmon farms.
 733 *PLoS ONE* **8**: e64039, doi:10.1371/journal.pone.0064039.
- 734 Anonymous. 2017a. *Akvakulturregisteret* (in Norwegian),

- 735 The Norwegian Ministry of Trade, Industry and Fish-
 736 eries, Oslo, [http://www.fiskeridir.no/Akvakultur/Registre-og-](http://www.fiskeridir.no/Akvakultur/Registre-og-skjema/Akvakulturregisteret)
 737 [skjema/Akvakulturregisteret](http://www.fiskeridir.no/Akvakultur/Registre-og-skjema/Akvakulturregisteret), downloaded 20th January 2017.
- 738 —. 2017b. *Fiskehelse (in Norwegian)*, Barentswatch,
 739 <https://www.barentswatch.no/fiskehelse/>.
- 740 Bricknell IR, Dalesman SJ, O'Shea B, Pert CC, Luntz AJ. 2006. Effect of envi-
 741 ronmental salinity on sea lice *Lepeophtheirus salmonis* settlement success. *Dis*
 742 *Aquat Organ* **71**: 201:2012, doi:10.3354/dao071201.
- 743 Brooks-Pollock E, Roberts GO, Keeling MJ. 2014. A dynamic model of
 744 bovine tuberculosis spread and control in Great Britain. *Nature* **511**,
 745 doi:10.1038/nature13529.
- 746 Byrd RH, Lu P, Nocedal J, Zhu C. 1995. A limited memory algorithm for bound
 747 constrained optimization. *SIAM Journal on Scientific Computing* **16**: 1190–
 748 1208.
- 749 Efron B, Tibshirani RJ. 1993. *An introduction to the bootstrap*, Chapman &
 750 Hall/CRC, Boca Raton.
- 751 Eichner C, Hamre LA, Nilsen F. 2015. Instar growth and molt increments in
 752 *Lepeophtheirus salmonis* (Copepoda: Caligidae) chalimus larvae. *Parasitology*
 753 *International* **64**: 86–96, doi:10.1016/j.parint.2014.10.006.
- 754 Forseth T, Barlaup BT, Finstad B, Fiske P, Gjøsæter H, Falkegård M, Hindar A,
 755 Mo TA, Rikardsen AH, Thorstad EB, Vøllestad V L. A. Wennevik. 2017. The
 756 major threats to Atlantic salmon in Norway. *ICES Journal of Marine Science*
 757 **74**: 1496–1513, doi:10.1093/icesjms/fsx020.

- 758 Grenfell BT, Wilson K, Isham VS, Boyd HEG, Dietz K. 1995. Modelling patterns
759 of parasite aggregation in natural populations: trichostrongylid nematode-
760 ruminant interactions as a case study. *Parasitology* **111** (Suppl.): S135–S51.
- 761 Hamre LA, Eichner C, Caipang CMA, Dalvin ST, Bron JE, Nilsen F, Boxshall G,
762 Skern-Mauritzen R. 2013. The salmon louse *Lepeophtheirus salmonis* (Cope-
763 poda:Caligidae) life cycle has only two chalimus stages. *PLoS ONE* **8**: e73539.
- 764 Irvine RJ, Stien A, Halvorsen O, Langvatn R, Albon SD. 2000. Life-history strate-
765 gies and population dynamics of abomasal nematodes in Svalbard reindeer
766 (*Rangifer tarandus plathyrrhynchus*). *Parasitology* **120**: 297–311.
- 767 Jansen P, Kristoffersen AB, Viljugrein H, Jimenez D, Aldrin M, Stien A. 2012.
768 Sea lice as a density dependent constraint to salmonid farming. *Proc R Soc B*
769 Doi:10.1098/rspb.2012.0084.
- 770 Jansen PA, Grøntvedt RN, Tarpai A, Helgesen KO, Horsberg TE. 2016.
771 Surveillance of the Sensitivity towards Antiparasitic Bath-Treatments in
772 the Salmon Louse (*Lepeophtheirus salmonis*). *PLoS ONE* **11**: e0149006,
773 doi.org/10.1371/journal.pone.0149006.
- 774 Kristoffersen AB, Qviller L, Helgesen KO, Vollset KW, Viljugrein H, Jansen
775 PA. 2017. Quantitative risk assessment of salmon louse-induced mortality of
776 seaward-migrating post-smolt Atlantic salmon. *Epidemics* Available online 2
777 December 2017, doi:10.1016/j.epidem.2017.11.001.
- 778 Liu YJ, Bjelland HV. 2014. Estimating costs of sea lice control strat-
779 egy in Norway. *Preventive Veterinary Medicine* **117**: 469–477,
780 doi:10.1016/j.prevetmed.2014.08.018.

- 781 Pawitan Y. 2001. *In all likelihood - statistical modelling and inference using*
 782 *likelihood*, Oxford, UK: Crarendon Press.
- 783 Pettersen JM, Brynildsrud OB, Huseby RB, Rich K, Aunsmo A, Jensen BB,
 784 Aldrin M. 2016. The epidemiological and economic effects from systematic
 785 depopulation of Norwegian marine salmon farms infected with pancreas disease
 786 virus. *Preventive Veterinary Medicine* **132**: 113–124.
- 787 Salama N, Murray A, Rabe B. 2016. Simulated environmental transport dis-
 788 tances of *Lepeophtheirus salmonis* in Loch Linnhe, Scotland, for informing
 789 aquaculture area management structures. *Journal of Fish Diseases* **39**: 419–
 790 428, doi:10.1111/jfd.12375.
- 791 Samsing F, Oppedal F, Dalvin S, Johnsen I, Vågseth T, Dempster T.
 792 2016. Salmon lice (*Lepeophtheirus salmonis*) development times, body size,
 793 and reproductive outputs follow universal models of temperature depen-
 794 dence. *Canadian Journal of Fisheries and Aquatic Science* **73**: 1841–1851,
 795 doi:10.1139/cjfas-2016-0050.
- 796 Stien A, Bjørn PA, Heuch PA, Elston DA. 2005. Population dynamics of salmon
 797 lice *Lepeophtheirus salmonis* on Atlantic salmon and sea trout. *Mar Ecol Prog*
 798 *Ser* **290**: 263–275.
- 799 Taranger G, Karlsen Ø, Bannister R, Glover K, Husa V, Karlsbakk E, Kvamme
 800 B, Boxaspen K, Bjørn P, Finstad B, Madhun A, Morton H, Svåsand T. 2015.
 801 Risk assessment of the environmental impact of Norwegian Atlantic salmon
 802 farming. *ICES Journal of Marine Science* **72**: 997–1021.
- 803 Tildesley MJ, Smith G, Keeling MJ. 2012. Modeling the spread and control of

804 foot-and-mouth disease in Pennsylvania following its discovery and options for
805 control. *Prev. Vet. Med.* **104**: 224–239.

806 Torrissen O, Jones S, Asche F, Guttormsen A, Skilbrei OT, Nilsen F, Horsberg
807 TE, Jackson D. 2013. Salmon lice – impact on wild salmonids and salmon
808 aquaculture. *Journal of Fish Diseases* **36**: 171–194, doi:10.1111/jfd.12061.

809 Zuur AF, Ieno EN, Walker N, Saveliev AA, Smith GM. 2009. *Mixed Effects Models*
810 *and Extensions in Ecology with R*, Springer, 1st ed., 574 p., doi:10.1007/978-
811 0-387-87458-6.

- A partly stage-structured model for salmon lice in a network of fish farms is introduced
- Adult females lice and other mobile stage are treated separately
- The time for recruitment of other mobile lice from the previous generation adult females increases by increasing temperatures
- The infection pressure from neighbouring farms decreases by increasing seaway distances to the neighbours
- The model can be used for prediction and for scenario simulations

Accepted Manuscript